PHYSICAL REVIEW B **72**, 014511 (2005)

Role of Ag doping in Ba_8Si_{46} compounds

N. Kamakura,[1] T. Nakano,[2] Y. Ikemoto,[3] M. Usuda,[4] H. Fukuoka,[5] S. Yamanaka,[5,6] S. Shin,[1] and K. Kobayashi[3]
[1]*Soft X-ray Spectroscopy Laboratory, RIKEN/SPring-8, Mikazuki, Hyogo 679-5148, Japan*
[2]*Department of Physics, Graduate School of Science, Osaka University, Toyonaka, Osaka 560-0043, Japan*
[3]*JASRI/SPring-8 Mikazuki, Hyogo 679-5198, Japan*
[4]*JAERI/SPring-8 Mikazuki, Hyogo 679-5198, Japan*
[5]*Department of Applied Chemistry, Graduate School of Engineering, Hiroshima University, Higashi-Hiroshima 739-8527, Japan*
[6]*CREST, Japan Science and Technology Corporation (JST), Kawaguchi 332-0012, Japan*
(Received 7 January 2005; revised manuscript received 1 April 2005; published 7 July 2005)

The silicon clathrate compound Ba_8Si_{46} shows superconductivity below the critical temperature (T_c) of 8 K, and the T_c decreases monotonically with doping Ag. In order to reveal effects of Ag doping on the electronic states, we have applied soft x-ray photoemission spectroscopy to Ag-doped silicon clathrate compounds $Ba_8Ag_xSi_{46-x}$ ($x=0,1,3,6$). The valence band photoemission spectra show that a Ba $5d$-derived state at the Fermi level (E_F), which is prominently observed in Ba_8Si_{46}, decreases with increasing Ag content. The reduction in the peak intensity at E_F with increasing Ag content is therefore in accord with the decrease of T_c in $Ba_8Ag_xSi_{46-x}$. Band structure calculation using local-density approximation reproduces the observed valence band spectra of $x=0$ and 6. The Si $2p$ and Ba $4d$ core-level photoemission spectra demonstrate that the valence electron of Si is attracted to the Ag site in $x=1$ and the $5d$ electron of Ba inside the Si_{24} cage is further donated to Ag in $x \geqslant 3$. Hence, Ag doping leads to the reduction of the peak at E_F.

DOI: 10.1103/PhysRevB.72.014511 PACS number(s): 74.70.Wz, 79.60.−i, 74.25.Jb, 74.62.Dh

Studies on silicon clathrate compounds trace back to discussion on the metal-insulator transition in Na_xSi_{46} and Na_xSi1_{36}.[1] Recently, $Na_2Ba_6Si_{46}$ and Ba_8Si_{46} have been found to show superconductivity with T_c of 4 and 8 K, respectively,[2–9] which have led to much notice into Si clathrate compounds. In Ba_8Si_{46}, Si atoms form a network consisting of Si_{24} and Si_{20} cages and Ba atoms are located at the centers of these Si cages (Fig. 1). Ba_8Si_{46} is similar to alkali-metal doped C_{60} materials in terms of a polyhedra-network system showing superconductivity.[10–15] In the C_{60} materials, the polyhedra are held together by van der Waals–type interactions. The superconductivity in the alkali-metal-doped C_{60} materials is based on the competition between the on-site Coulomb repulsion energy among the electrons occupying t_{1u}-derived C_{60} bands and the coupling between these electrons and intramolecular vibrations of C_{60}. In Si clathrate compounds, however, the polyhedra share the pentagonal and hexagonal faces as shown in Fig. 1 and form a covalently bonded network. The band structure calculation by the density functional theory for Ba_8Si_{46} has predicted that strong hybridization between the Si $3p$ and Ba $5d$ states modifies the density of states (DOS) of the Si network and forms a narrow peak at the E_F.[7,16,17] This hybridized state at E_F is thought to play a crucial role in the superconductivity of Ba_8Si_{46}, since T_c is a function of DOS at E_F in normal state $[N(E_F)]$ through the coupling constant $\lambda=N(E_F)V$, where V is electron-excitation coupling strength.[18] The photoemission spectroscopy using He Iα (21.218 eV) and He IIα (40.814 eV) has shown the narrow peak at E_F and has observed the superconducting gap $[2\Delta(E_F)/k_BT_c]$ of 4.38 in the superconducting state.[19] The hybridized state at E_F has been also observed by the Knight shift in nuclear magnetic resonance (NMR)[20,21] and the specific-heat and magnetic susceptibility measurements.[5] On the other hand, the study by neutron scattering and extended x-ray absorption fine structure (EXAFS) has shown that the vibrational coupling between Ba and Si network inside the Si_{24} cage is also the important parameter to explain consistently the superconductivity in Ba_8Si_{46} and the absence of superconductivity in Na_8Si_{46} for which $N(E_F) \neq 0$.[22] The recent study on the isotope effect in Raman spectrum has indicated that the superconductivity in Ba_8Si_{46} is explained by Bardeen-Cooper-Schrieffer (BCS) mechanism with medium coupling regime.[5]

In $Ba_8Ag_xSi_{46-x}$ studied here, Si atoms are replaced with Ag atoms at 6c sites which belong only to the Si_{24} cages. The 6c sites are represented by black circles in Fig. 1 which shows the crystal structure of $Ba_8Ag_xSi_{46-x}$. In $Ba_8Ag_3Si_{43}$, Ag atoms occupy the 6c sites alternately in the Si sixfold ring. $Ba_8Ag_xSi_{46-x}$ shows the superconductivity in $x \leqslant 3$, while the T_c decreases with increasing Ag content to 7 K and 2.8 K for $x=1$ and 3, respectively. The superconductivity has not been observed down to 1.8 K in Ag-doped clathrates with $x>3$.[23] Therefore, the systematic study for the elec-

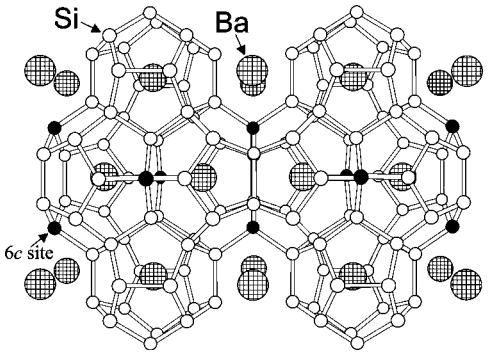

FIG. 1. Crystal structure of $Ba_8Ag_xSi_{46-x}$. Black circles indicate the 6c sites where Si atom is replaced with Ag atom by Ag doping.

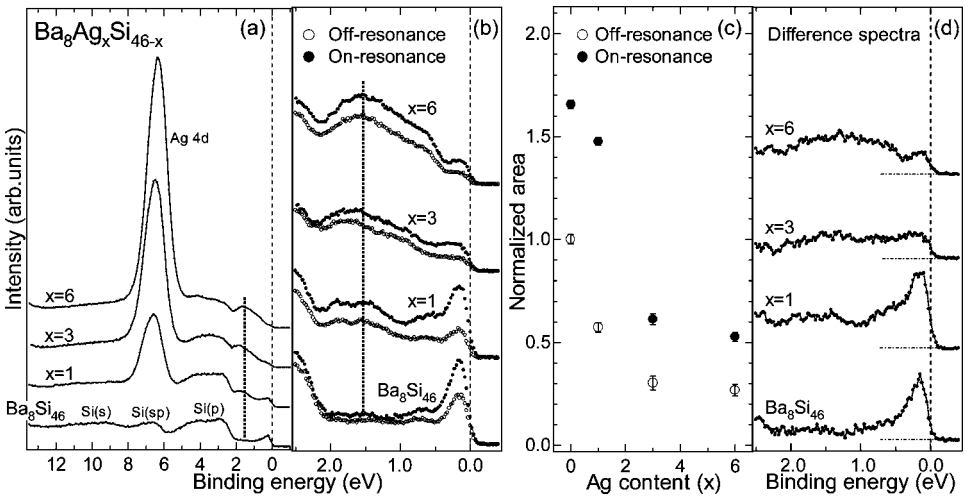

FIG. 2. (a) The valence band spectra of $Ba_8Ag_xSi_{46-x}$ ($x=0,1,3,6$), measured with $h\nu=780$ eV. The spectra are normalized by the intensity at 12.0 eV. (b) Resonant photoemission spectra at Ba $3d$ threshold. The closed and open circles show the on-resonant ($h\nu=789$ eV) and off-resonant ($h\nu=780$ eV) spectra of $Ba_8Ag_xSi_{46-x}$ ($x=0,1,3,6$). The spectra are normalized by the photon flux. (c) The areas under the curves between E_F and 0.35 eV of the on- and off-resonant spectra shown in (b) are plotted by the closed and open circles with error bars, respectively. All values are normalized by the value for the off-resonant spectrum of Ba_8Si_{46}. (d) The difference spectra between the on- and off-resonance spectra of $Ba_8Ag_xSi_{46-x}$ ($x=0,1,3,6$).

tronic states of $Ba_8Ag_xSi_{46-x}$ as a function of Ag content (x) provides the important knowledge on the superconductivity in Si clathrate compounds such as the mechanism of the change in the T_c and the appearance and absence of the superconductivity, which are indeed related to the behavior of the DOS at E_F. Here, in order to study the electronic states of $Ba_8Ag_xSi_{46-x}$ depending on Ag content (x) and to elucidate the change in them caused by Ag doping, we have applied soft x-ray photoemission to $Ba_8Ag_xSi_{46-x}$ with $x=0$, 1, 3, and 6. An advantage in the use of soft x-ray is a long photoelectron mean free path compared to the photoemission using ultraviolet rays and, hence, the effective probe of bulk electronic states. The valence band photoemission has probed the DOS at E_F depending on Ag content and has shown the additional bonding states at $\sim$1.5 eV binding energy in Ag-doped Si clathrates. In addition, the resonant photoemission at Ba $3d$ threshold, which enhances the Ba states selectively, has been performed to study the partial density of states (pDOS) of Ba in the valence band. Ba $4d$ and Si $2p$ core-level photoemission have been also done to study the electronic states of $Ba_8Ag_xSi_{46-x}$ ($x=0,1,3,6$) with element specification. These core-level spectra elucidate the interchange of the charge between the elements and the origin of changes in the valence band.

$Ba_8Ag_xSi_{46-x}$ ($x=0,1,3,6$) were prepared under high pressure.[4,6,7,23] Ba, Si, and Ag were mixed at the given composition and melted in an arc furnace under Ar atmosphere. The melted mixtures were ground and compressed at 3 GPa and 800 °C in an h-BN container. The photoemission experiment was performed at the twin-helical undulator beamline BL25SU of SPring-8, which was equipped with a SCIENTA SES 200 analyzer.[24] The samples were fractured and measured in vacuum better than 3×10^{-10} Torr at 20 K. Electronic band structure calculations of Ba_8Si_{46} and $Ba_8Ag_6Si_{40}$ were performed using the full-potential linearized augmented-plane-wave (FLAPW) method[25–27] based on the density-functional theory with the LDA.

Figure 2(a) shows the valence band spectra of $Ba_8Ag_xSi_{46-x}$ ($x=0,1,3,6$) measured with $h\nu=780$ eV. The off-resonant valence band spectra are predominantly contributed by the Si states owing to the large proportion of Si in $Ba_8Ag_xSi_{46-x}$. The spectral structures at $\sim$2–5, 6–8, and 8–12 eV in the spectrum of Ba_8Si_{46} correspond to the Si $3p$, $3sp$, and $3s$ states, respectively, which are clearly observed in this spectrum, and a sharp peak is observed at E_F. By Ag doping, the Ag $4d$ peak arises at $\sim$6.5 eV in the valence band and increases the intensity in keeping with Ag content. In addition, the peak intensity at E_F decreases with increasing Ag content and additional states grow at $\sim$1.5 eV, that can be considered bonding states with Ag. In Fig. 2(b), the valence band spectra are measured in the energy range up to 2.5 eV to see the electronic states near E_F in more detail. The on-resonant photoemission spectra ($h\nu=789$ eV) at the Ba $3d$ threshold were also shown in Fig. 2(b) by closed circles to study the contribution of Ba states to the valence band. In the off-resonant spectra shown by open circles in Fig. 2(b), the sharp peak at E_F is clearly seen in Ba_8Si_{46} and drastically decreases the intensity with increasing Ag content. The additional structure is also clear in Fig. 2(b). The structure at $\sim$1.5 eV which is not observed in Ba_8Si_{46} appears in $Ba_8Ag_1Si_{45}$ and increases the intensity in keeping with Ag content.

To estimate the $N(E_F)$, area under the curve up to 0.35 eV is evaluated from the off-resonant spectra of $Ba_8Ag_xSi_{46-x}$ ($x=0,1,3,6$). The areas normalized by the value for Ba_8Si_{46} are estimated at 1, 0.573, 0.303, and 0.268 for $x=0$, 1, 3, and 6, respectively, which are plotted in Fig. 2(c) by open circles. Since $N(E_F)$ for Ba_8Si_{46} was reported to be 31 states per eV per Si_{46} by the specific-heat measurement[5] $N(E_F)$ for $x=1$, 3, and 6 are estimated at 17.8, 9.4, and 8.3 states per eV per Si_{46}, respectively. Compared to $N(E_F)$ in alkali-metal doped C_{60} materials which have been reported as $N(E_F)=8.5$ and 10 per eV per C_{60} for K_3C_{60} and Rb_3C_{60} in Ref. 28, respec-

tively, the values for $Ba_8Ag_xSi_{46-x}$ are quite large in $x \leqslant 1$ and equivalent in $x \geqslant 3$. It shows that the large DOS at E_F is characteristic of $Ba_8Ag_xSi_{46-x}$ with small x and plays the important role in the appearance of the superconductivity. The BCS theory states that T_c shows the exponential decrease against $1/\lambda$.[18] Hence, the reduction of $N(E_F)$ in keeping with the T_c is qualitatively consistent with the BCS theory. In $Ba_8Ag_xSi_{46-x}$, the reduction of $N(E_F)$ is the dominant factor causing the decrease of the T_c with the increase of Ag content. However, although the finite DOS still exists at E_F $[N(E_F) \neq 0]$, no superconductivity is observed in $Ba_8Ag_6Si_{40}$, which may indicate that the vibrational coupling between Ba and cages consisting of Si and Ag weakens in $x=6$.

In the on-resonant spectra of Ba_8Si_{46} and $Ba_8Ag_1Si_{45}$, the peak at E_F is markedly enhanced. In particular, the enhancement in the on-resonant spectrum of Ba_8Si_{46} is restricted within the narrow energy range up to ~0.8 eV, which is also found by the sharp pDOS of Ba at E_F in the difference spectrum [Fig. 2(d)] between on- and off-resonant spectra. It shows that the delocalized 6s state that is occupied by two electrons in the configuration of atomic Ba is not occupied in Ba_8Si_{46}. Part of these two electrons occupy the Ba 5d state to form the narrow hybridized peak at E_F together with Si 3p, and the residual electrons are donated to the Si sites in Ba_8Si_{46}. In Fig. 2(c), areas under the curves up to 0.35 eV for the on-resonant spectra are also plotted by closed circles, which show the enhancement of 65.5% in the on-resonance over the off-resonance for Ba_8Si_{46}. Ba-doped fullerene Ba_6C_{60}, which exhibits the superconductivity below 7 K,[29] also shows the peak near E_F originated by the hybridization between Ba 5d and t_{1u} and t_{1g} orbitals of C_{60}.[30,31] The resonant photoemission for Ba_6C_{60} has shown the ~25% resonant enhancement of Ba states the peak near E_F.[30] Therefore, the proportion of the Ba 5d in the peak at E_F is much larger in Ba_8Si_{46} than in Ba_6C_{60}. This comparison verifies that the strong hybridization with Ba 5d causes the large DOS of $Ba_8Ag_xSi_{46-x}$ $(x=0)$. As found by Fig. 2(c), the enhancement near E_F in the on-resonant spectrum of $Ba_8Ag_1Si_{45}$ over the off-resonant spectrum is larger than that of Ba_8Si_{46}. The difference spectra [Fig. 2(d)] also show the larger intensity near E_F in $Ba_8Ag_1Si_{45}$ than in Ba_8Si_{46}. Furthermore, the enhancement in the on-resonant spectrum for $Ba_8Ag_1Si_{45}$ spreads in wider energy range [Fig. 2(b)]. It indicates that, in $Ba_8Ag_1Si_{45}$, delocalized Ba 6s states are partially occupied in addition to the Ba 5d state. This additional occupation into the Ba 6s also contributes to the increase of the Ba pDOS (the intensity of the difference spectrum) near E_F.[32] The off-resonant spectrum of $Ba_8Ag_1Si_{45}$, on the other hand, shows the much lower intensity near E_F than that of Ba_8Si_{46}, which indicates the decrease of Si pDOS near E_F in $Ba_8Ag_1Si_{45}$. The decrease of the Si pDOS in $Ba_8Ag_1Si_{45}$ can be understood by the polar character of the Ag-Si bond,[33] which will be also discussed in the Si 2p core-level photoemission. In Ag-doped Si clathrates with $x \geqslant 3$, strong resonance is not observed near E_F but weak enhancement in the on-resonant spectra still remains in the wide energy range including the additional states at ~1.5 eV and the reduced peak at E_F [Fig. 2(b)]. The difference spectra of $x \geqslant 3$ in Fig. 2(d) also show that there exists the low intensity in the energy range between E_F and 2.5 eV. It indicates that the Ba 5d electron, which forms the large Ba pDOS at E_F and derives the hybridization forming the large DOS at E_F in $x \leqslant 1$, is attracted to the Ag sites, while the delocalized Ba 6s is left in the valence band. As the result that the hybridization with Ba 5d state weakens, the DOS near E_F decreases further with the increase of Ag content in $x \geqslant 3$.

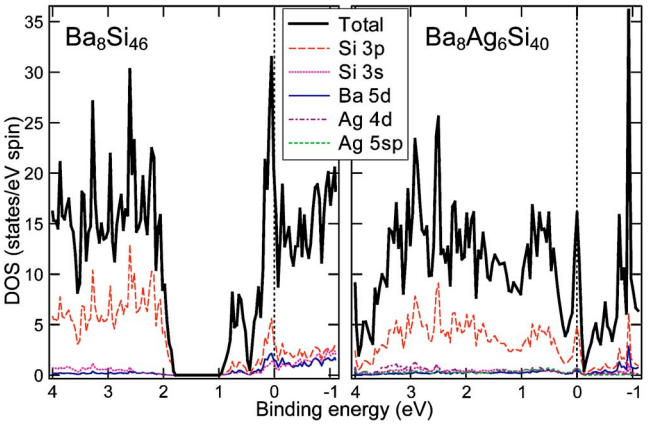

FIG. 3. (Color online.) Total and partial DOS of Ba_8Si_{46} and $Ba_8Ag_6Si_{40}$ by the LDA calculation.

In Figs. 3(a) and 3(b), the (p)DOS by LDA calculation are shown for Ba_8Si_{46} and $Ba_8Ag_6Si_{40}$, respectively. The LDA calculation reproduces the drastic change of the observed valence band from Ba_8Si_{46} to $Ba_8Ag_6Si_{40}$. For Ba_8Si_{46}, the sharp peak at E_F and little DOS between 1 and 2 eV shown in Fig. 2 are consistent with the calculation in Fig. 3(a). The calculation also reproduces the observed spectrum of $Ba_8Ag_6Si_{40}$, that is, the decrease of the peak at E_F and additional states between 1 and 2 eV. In the calculation for $Ba_8Ag_6Si_{40}$, the sharp DOS which show the large contribution from Ba 5d is expected to be located above E_F (~−1 eV). Hence, a part of the DOS at the E_F in Ba_8Si_{46} moves above E_F in $Ba_8Ag_6Si_{40}$ and the other forms the bonding states located at the energy range between the peak at E_F and Si 3p state.

Figure 4(a) shows the Ba 4d core-level spectra of $Ba_8Ag_xSi_{46-x}$ $(x=0,1,3,6)$. The Ba 4d spectra reveal the two sets of spin-orbit splitting peaks which is labeled as A and B in Fig. 4(a). It is found by the intensity ratio beween A and B that the main peaks A at 89.7 eV and 92.4 eV are originated by Ba inside the Si_{24} cage (six sites in Si_{46} unit) and smaller peaks B at 89.2 and 91.8 eV come from Ba inside the Si_{20} cage (two sites in Si_{46} unit). Hence, the valence of Ba is not homogeneous between Si_{24} and Si_{20} cages, but depends on the number of surrounding Si atoms. In the Ba_6C_{60} mentioned above, Ba is thought to be monovalent,[31] which indicates that the valence of Ba deviates from the limit of complete (two electrons) charge transfer from 6s because t_{1u} and t_{1g} orbitals of C_{60} are hybridized with Ba 5d state. The peak position of Ba $4d_{5/2}$ in Ba_6C_{60} has been ~89.8 eV,[30] which is approximately equal to the peak position A (89.725 eV) of Ba $4d_{5/2}$ in Ba_8Si_{46}. Therefore, Ba inside the Si_{24} cage in Ba_8Si_{46} possibly shows the configuration similar to Ba in Ba_6C_{60}. The low-energy component B originated by Ba inside the Si_{20} cage shows that the valence (the number of

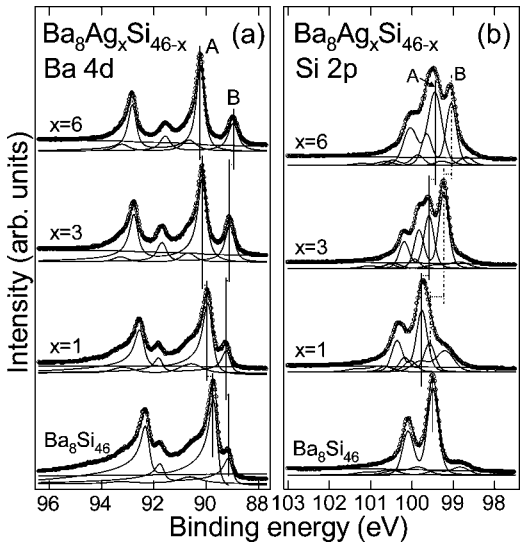

FIG. 4. (a) The open circles show the Ba 4*d* spectra of $Ba_8Ag_xSi_{46-x}$ ($x=0,1,3,6$), measured with $h\nu=815$ eV. The fitting results are shown by the solid lines, which consist of three components. The peaks marked with A and B in the figure are derived from Ba inside the Si_{24} and Si_{20} cages, respectively. The broad component corresponds to the contribution of the surface. (b) The open circles show the Si 2*p* spectra of $Ba_8Ag_xSi_{46-x}$ ($x=0,1,3,6$) measured with $h\nu=815$ eV. The fitting curves are shown by the solid lines. In the spectra of Ag-doped Si clathrates, the main components are marked by A and B.

occupied 5*d* electrons) of Ba inside the Si_{20} cage is more than that of Ba inside the Si_{24} cage for Ba_8Si_{46} in which only the Ba 5*d* state is partially occupied. Hence, the Ba 5*d* electrons used for the hybridization at the Si_{20} cage are more than that at the Si_{24} cage. This excess electron at Ba inside the Si_{20} cage causes the large enhancement of the on-resonant valence band spectrum in Ba_8Si_{46} compared to that in Ba_6C_{60}. With increasing Ag content, peak A shifts to higher binding energy and peak B shifts to lower binding energy, while the peak B in $Ba_8Ag_1Si_{45}$ slightly shifts to higher binding energy than that in Ba_8Si_{46} in contrast to the shift of peak B in $x\geqslant 3$. The high binding energy shifts of both the peaks in $Ba_8Ag_1Si_{45}$ may indicate that the less occupation of the Ba electrons at the Si_{24} and Si_{20} cages in $Ba_8Ag_1Si_{45}$ than in Ba_8Si_{46}. The on-resonant spectrum of $Ba_8Ag_1Si_{45}$, however, shows that the delocalized Ba 6*s* state is added in the valence band. This behavior in the valence band is consistently explained by the characteristic feature of Ba core level. The Ba 4*d* core level is probably more sensitive to the variation in the number of 5*d* electrons than that of the 6*s* electrons as has been interpreted in Refs. 34–36, since the Ba 5*d* orbitals have smaller radial extent than the delocalized 6*s* orbital. Hence, the shifts of the peaks A and B in the Ba 4*d* spectrum of $Ba_8Ag_1Si_{45}$ are governed by the decrease of the 5*d* electron and insensitive to the change in the occupation of 6*s*. The high binding energy shifts for the peaks A and B of the Ba 4*d* spectrum and the broad enhancement of the on-resonant spectrum in $Ba_8Ag_1Si_{45}$, therefore, indicate that Ba in $Ba_8Ag_1Si_{45}$ loses the 5*d* electrons in the Si_{24} and Si_{20} cages and gains the 6*s* character in the valence band. As the result that the hybridization between Ba 5*d* and Si 3*p* weakens, Ba in $Ba_8Ag_1Si_{45}$ may show a configuration similar to atomic Ba.

In clathrates with $x\geqslant 3$, the observed core-level shift of peak A indicates that Ba inside the Si_{24} cages loses the 5*d* electrons further with increasing Ag content. The decrease of the Ba 5*d* electron at the Si_{24} cage can be understood by considering the interchange of the charge with doped Ag. Since Ag has greater electronegativity than Ba and Si,[33] the 5*d* electron of Ba inside the Si_{24} cage including doped Ag is attracted to the Ag site further. Therefore, the 5*d* electron of Ba inside the Si_{24} cage decreases selectively. The decrease of the Ba 5*d* electrons in Ag-doped clathrates with $x\geqslant 3$ is consistent with the resonant photoemission result, showing the reduction of the Ba 5*d* states at E_F with the increase of Ag content in $x\geqslant 3$. The shift of peak B is opposite to that of peak A in the Ba 4*d* spectra of $x\geqslant 3$. The difference between the valences of Ba in the Si_{24} and Si_{20} cages, therefore, becomes large with increasing Ag content. The shift of peak B in $x\geqslant 3$ indicates that the electrons that move to the Si network from Ba inside the Si_{24} cage through doped Ag are used for the hybridization between Si 3*p* and Ba 5*d* states at the Si_{20} cage in clathrates of $x\geqslant 3$. Nevertheless, the total number of Ba 5*d* electrons decreases with the increase of Ag content in $x\geqslant 3$ as observed in the resonant photoemission. Since the number of Ba atoms inside the Si_{24} cage (six sites in Si_{46} unit) is three times as large as that inside the Si_{20} cage (two sites in Si_{46} unit), the change in the valence of Ba inside the Si_{24} cage affects the valence band more strongly than that of Ba inside the Si_{20} cage. Furthermore, the decrease in the Ba 5*d* electron at the Si_{24} cage is larger than the increase in that at the Si_{20} cage, because the positive shift of peak A, which is +0.500 eV in $Ba_8Ag_6Si_{40}$ from the peak position in Ba_8Si_{46}, is larger than the negative shift of peak B which is −0.175 eV.

Another point to note is that the Ba 4*d* peak of Ba_8Si_{46} takes on an asymmetric shape, which can be distinguished by the tail extended up to the background, and becomes symmetric with doping Ag. An asymmetric line shape results from sharp cut off at E_F and is described by Doniach and Šunjić line shape.[37] To estimate the asymmetric parameter, a curve fitting was performed using the Doniach and Šunjić line shape.[37] The best fitting results are shown in Fig. 4(a) by solid curves. Each fitting result consists of three spin-orbit split curves; the two asymmetric curves correspond to the peaks due to Ba in the Si_{24} and Si_{20} cages, as already shown by A and B, respectively, and the other is the broad peak with smaller amount, which can be considered a surface component. The conclusive fitting curves match well with the photoemission spectra. The asymmetric parameters of peak A are estimated to be 0.375, 0.250, 0.130, and 0.080 for $x=0$, 1, 3, and 6 by the curve fitting, respectively. The systematic transformation of the Ba 4*d* spectra from asymmetric shape for Ba_8Si_{46} into more symmetric shape for $Ba_8Ag_6Si_{40}$ is consistent with the changes in the DOS at E_F and the T_c depending on Ag content.

Figure 4(b) shows the Si 2*p* spectra of $Ba_8Ag_xSi_{46-x}$ ($x=0,1,3,6$). Although the Si 2*p* spectra are complicated in Ag-doped clathrates, a curve fitting was attempted to understand the spectral features. In Ba_8Si_{46}, there are three unequal

sites, which are namely 24*k*, 16*i*, and 6*c* sites. The 6*c* site is the site which is represented by black circles in Fig. 1 and the 24*k* site is adjacent to the 6*c* site. The second nearest neighbor to the 6*c* site is the 16*i* site. In spite of the presence of these different Si sites, the Si 2*p* spectrum of Ba_8Si_{46} shows one bulk component with large intensity and small contributions located at the low and high binding energy sides to the main peak [Fig. 4(b)]. The only one large component in Si 2*p* spectrum indicates that the charge is homogeneously distributed on Si network in Ba_8Si_{46}, in contrast to the difference between the valences of Ba in the Si_{24} and Si_{20} cages. The fitting spectra for Ag-doped Si clathrates show two main components. Hence, Ag doping causes the Si atoms with two different valences. In Fig. 4(b) the main component at the high binding energy side is marked with A and that at the low binding energy side with B. In $Ba_8Ag_1Si_{45}$, peak A is located at higher binding energy than the main peak of Ba_8Si_{46}. The bonding between Ag and Si is expected to have the larger electron density at the Ag site because the electronegativity of Ag is still greater than that of Si.[33] Hence, the Si 2*p* spectrum of $Ba_8Ag_1Si_{45}$ shows the component which shifts to the higher binding energy. The peak shift of the Si 2*p* spectrum in $Ba_8Ag_1Si_{45}$ is consistent with the valence band spectrum of $Ba_8Ag_1Si_{45}$, which shows the drastic decrease in the *p*DOS of Si. In $x \geqslant 3$, on the other hand, the component (B), which greatly shifts to low binding energy, is observed in the Si 2*p* spectra. Since Ba provides the electrons for the Si network at the Si_{24} cage through doped Ag in $x \geqslant 3$ as was shown in the peak shift (A) of the Ba 4*d* spectra, the excess electron charge on Ag possibly causes conversion of the bonding character so as to provide the electrons for the Si network through Ag in $x \geqslant 3$. The provided electrons to Si sites are partially used for the hybridization with Ba at the Si_{20} cage as was shown by the shift of peak B in Ba 4*d* spectra and are probably also added to the bonding states at $\sim$1.5 eV in the valence band. Hence, complicated charge balance depending on Ag content results so as to stabilize $Ba_8Ag_xSi_{46-x}$ energetically. In $Ba_8Ag_6Si_{40}$, since all of the 6*c* sites are replaced with Ag atoms, the Si 2*p* spectrum is simply assigned by the Si sites. If components A and B are assumed to come from the 24*k* and 16*i* sites, the ratio between A and B is expected to be 0.6:0.4, which approximately matches with the intensity ratio 0.52:0.48 estimated by the curve fit in $Ba_8Ag_6Si_{40}$.

In conclusion, valence band and core-level photoemission using soft x rays have been applied to $Ba_8Ag_xSi_{46-x}$ ($x=0,1,3,6$). In the valence band spectra of Ba_8Si_{46}, a sharp peak was prominently observed at E_F. The resonant photoemission confirmed the strong hybridization with the Ba 5*d* state for this peak. The peak intensity at E_F decreases with increasing Ag content. In $Ba_8Ag_1Si_{45}$, the valence electron of Si is attracted to Ag, which causes the decrease in the DOS at E_F. The resonant photoemission and Ba 4*d* core-level spectrum have shown that the Ba 6*s* state admixes in the valence band of $Ba_8Ag_1Si_{45}$. In $x \geqslant 3$, conversion of the bonding character takes place. In contrast to $Ba_8Ag_1Si_{45}$, the 5*d* electron of Ba inside the Si_{24} cage is exclusively attracted to Ag in $x \geqslant 3$ and the DOS decreases further as the result that the hybridization with the Ba 5*d* state weakens. The excess electron charge on Ag flows to Si network. The electron-flow to Si network would form the additional bonding states at $\sim$1.5 eV with doped Ag. As the result of these interchanges of the charge between the elements of $Ba_8Ag_xSi_{46-x}$, Ag doping causes the decrease in the peak intensity at E_F, which is the dominant factor decreasing the T_c. The absence of superconductivity in $Ba_8Ag_6Si_{40}$ for which $N(E_F) \neq 0$ indicates the weak vibrational coupling between Ba and cages consisting of Si and Ag in $Ba_8Ag_6Si_{40}$. The change of the valence band by Ag doping was consistent with the LDA calculation. $Ba_{8-x}Si_{46}$ (Refs. 6 and 7) and $Na_xBa_{8-x}Si_{46}$ (Refs. 2 and 3) in which Ba atoms are deintercalated and partially replaced by Na atoms, respectively, and $Ba_8Si_{46-x}Ge_x$ (Ref. 38) in which Si atoms are partially replaced with Ge atoms also show the variation of T_c. Therefore, the experimental studies of the electronic states for these systems are desirable for understanding the overall mechanism on the appearance of the narrow peak at E_F and superconductivity in Si clathrate compounds.

We would like to thank Dr. T. Muro and Dr. FZ. Guo for help with our work. One of the authors (M.U.) would like to thank Professor N. Hamada for allowing us to use his FLAPW code.

[1] N. F. Mott, J. Solid State Chem. **6**, 348 (1973).
[2] H. Kawaji, H. O. Horie, S. Yamanaka, and M. Ishikawa, Phys. Rev. Lett. **74**, 1427 (1995).
[3] S. Yamanaka, H. Horie, H. Nakano, and M. Ishikawa, Fullerene Sci. Technol. **3**, 21 (1995).
[4] S. Yamanaka, E. Enishi, H. Fukuoka, and M. Yasukawa, Inorg. Chem. **39**, 56 (2000).
[5] K. Tanigaki, T. Shimizu, K. M. Itoh, J. Teraoka, Y. Moritomo, and S. Yamanaka, Nat. Mater. **2**, 653 (2003).
[6] H. Fukuoka, J. Kiyoto, and S. Yamanaka, Inorg. Chem. **42**, 2933 (2003).
[7] H. Fukuoka, J. Kiyoto, and S. Yamanaka, J. Phys. Chem. Solids **65**, 333 (2004).
[8] S. L. Fang, L. Grigorian, P. C. Eklund, G. Dresselhaus, M. S. Dresselhaus, H. Kawaji, and S. Yamanaka, Phys. Rev. B **57**, 7686 (1998).
[9] T. Kume, H. Fukuoka, T. Koda, S. Sasaki, H. Shimizu, and S. Yamanaka, Phys. Rev. Lett. **90**, 155503 (2003).
[10] C. T. Chen, L. H. Tjeng, P. Rudolf, G. Meigs, J. E. Rowe, J. Chen, J. P. McCauley Jr, A. B. Smith III, A. R. McGhie, W. J. Romanow, and E. W. Plummer, Nature (London) **352**, 603 (1991).
[11] P. J. Benning, José Luís Martins, J. H. Weaver, L. P. F. Chibante, and R. E. Smalley, Science **252**, 1417 (1991).
[12] G. K. Wertheim, J. E. Rowe, D. N. E. Buchanan, E. E. Chaban, A. F. Hebard, A. R. Kortan, A. V. Makhija, and R. C. Haddon, Science **252**, 1419 (1991).

[13] T. Takahashi, S. Suzuki, T. Morikawa, H. Katayama-Yoshida, S. Hasegawa, H. Inokuchi, K. Seki, K. Kikuchi, S. Suzuki, K. Ikemoto, and Y. Achiba, Phys. Rev. Lett. **68**, 1232 (1992).
[14] M. Knupfer, M. Merkel, M. S. Golden, J. Fink, O. Gunnarsson, and V. P. Antropov, Phys. Rev. B **47**, R13 944 (1993).
[15] S. Saito and A. Oshiyama, Phys. Rev. B **44**, R11 536 (1991).
[16] S. Saito and A. Oshiyama, Phys. Rev. B **51**, R2628 (1995).
[17] K. Moriguchi, M. Yonemura, A. Shintani, and S. Yamanaka, Phys. Rev. B **61**, 9859 (2000).
[18] M. Tinkham, *Introduction to Superconductivity* (McGraw-Hill, New York, 1975).
[19] T. Yokoya, A. Fukushima, T. Kiss, K. Kobayashi, S. Shin, K. Moriguchi, A. Shintani, H. Fukuoka, and S. Yamanaka, Phys. Rev. B **64**, 172504 (2001).
[20] Y. Maniwa, H. Sakamoto, H. Tou, Y. Aoki, H. Sato, F. Shimizu, H. Kawaji, and S. Yamanaka, Mol. Cryst. Liq. Cryst. Sci. Technol., Sect. A **341**, 497 (2000).
[21] H. Sakamoto, H. Tou, H. Ishii, Y. Maniwa, E. A. Reny, and S. Yamanaka, Physica C **341**, 2135 (2000).
[22] E. Reny, A. SanMiguel, Y. Guyot, B. Masenelli, P. Melinon, L. Saviot, S. Yamanaka, B. Champagnon, C. Cros, M. Pouchard, M. Borowski, and A. J. Dianoux, Phys. Rev. B **66**, 014532 (2002).
[23] Y. Nozue, G. Hosaka, E. Enishi, and S. Yamanaka, Mol. Cryst. Liq. Cryst. Sci. Technol., Sect. A **341**, 1313 (2000).
[24] Y. Saitoh, T. Nakatani, T. Matsushita, T. Miyahara, M. Fujisawa, K. Soda, T. Muro, S. Ueda, H. Harada, A. Sekiyama, S. Imada, H. Daimon, and S. Suga, J. Synchrotron Radiat. **5**, 542 (1998).
[25] T. Takeda and J. Kübler, J. Phys. F: Met. Phys. **9**, 661 (1979).
[26] H. J. F. Jansen and A. J. Freeman, Phys. Rev. B **30**, 561 (1984).
[27] S. H. Vosko, L. Wilk, and M. Nusair, Can. J. Phys. **58**, 1200 (1980).
[28] S. Satpathy, V. P. Antropov, O. K. Andersen, O. Jepsen, O. Gunnarsson, and A. I. Liechtenstein, Phys. Rev. B **46**, 1773 (1992).
[29] A. R. Kortan, N. Kopylov, S. Glarum, E. M. Gyorgy, A. P. Ramirez, R. M. Flemming, O. Zhou, F. A. Thiel, P. L. Trevor, and R. C. Haddon, Nature (London) **360**, 566 (1992).
[30] M. Knupfer, F. Stepniak, and J. H. Weaver, Phys. Rev. B **49**, 7620 (1994).
[31] Th. Schedel-Niedrig, M. C. Bohm, H. Werner, J. Schulte, and R. Schlogl, Phys. Rev. B **55**, 13 542 (1997).
[32] The *p*DOS of Ba 5*d*, however, decreases in $Ba_8Ag_1Si_{45}$ owing to the change in the occupied Ba state from 5*d* to the admixture of 6*s* character, as shown in the Ba 4*d* core-level photoemission. The larger intensity in the difference spectrum of $Ba_8Ag_1Si_{45}$ than that of Ba_8Si_{46} in the energy range up to 2.5 eV likely results from the different extent of the enhancement between Ba 5*d* and 6*s* states in the on-resonance, while the variation in the total electron count of Ba in the valence band also influences the enhancement in the on resonance.
[33] L. Pauling, *The Nature of the Chemical Bond* (Cornell University, Ithaca, NY, 1960).
[34] G. K. Wertheim, J. Electron Spectrosc. Relat. Phenom. **34**, 309 (1984).
[35] M. E. Preil, J. E. Fischer, S. B. DiCenzo, and G. K. Wertheim, Phys. Rev. B **30**, R3536 (1984).
[36] In-Sang Yang, A. G. Schrott, and C. C. Tsuei, Phys. Rev. B **41**, 8921 (1990).
[37] S. Doniach and M. Šunjić, J. Phys. C **3**, 285 (1970).
[38] H. Fukuoka, J. Kiyoto, and S. Yamanaka, J. Solid State Chem. **175**, 237 (2003).